Superconducting properties of layered $Nb_{0.53}Ti_{0.47}$/Ge structures prepared by dc sputtering

B. Y. Jin, Y. H. Shen, H. Q. Yang, H. K. Wong, J. E. Hilliard, and J. B. Ketterson
Materials Research Center, Northwestern University, Evanston, Illinois 60201

I. K. Schuller
Argonne National Laboratory, Argonne, Illinois 60439

(Received 13 September 1984; accepted for publication 14 November 1984)

Sandwich and superlattice structures composed of the high critical field superconducting alloy $Nb_{0.53}Ti_{0.47}$ (where the compositions refer to weight percent) and amorphous Ge were sputter-deposited on sapphire substrates using a novel multi-sputter-gun system. The thicknesses of both the superconducting $Nb_{0.53}Ti_{0.47}$ and the insulating Ge layers were varied over a wide range in order to study the two-dimensional (2D) and three-dimensional (3D) superconducting properties of these structures. The observed suppression of the measured resistive superconducting transition temperature T_c with increasing sheet resistance is tentatively interpreted using the Maekawa–Fukuyama theory which incorporates contributions from localization and Coulomb interaction effects. The upper critical fields, with the field both normal $H_{c2\perp}$ and parallel $H_{c2\parallel}$ to the film, were measured up to 50 kG. $H_{c2\parallel}$ exhibited 2D behavior when the thickness of the superconducting layer was less than 200 Å. The zero temperature values of $H_{c2\parallel}(0)$ were estimated using the Rickayzen formula, which is valid in the regime $l \ll (l\xi_0)^{1/2} \ll D_s$ (where l, ξ_0, and D_s are the mean free path, pure material coherence length, and film thickness, respectively). The estimated $H_{c2\parallel}(0)$ peaks at about 400 kG for a superconducting layer thickness of 144 Å. This rather high upper critical field, which is considerably above the bulk value of 145 kG, likely has its origin in flux line accommodation within the insulating Ge layers. Since the Rickayzen expression neglects paramagnetic limiting, the true $H_{c2\parallel}(0)$ is expected to be somewhat lower; localization/interaction and spin orbit coupling effects are also neglected in this treatment. The situation is none the less encouraging and suggests multilayer superconductors may have a place in high-field magnet technology.

I. INTRODUCTION

The results of Gamble *et al.*,[1] on the highly anisotropic superconducting properties of the layered dichalcogenides (transition-metal dichalcogenides intercalated with organic molecules), aroused considerable interest, both theoretically[2–5] and experimentally,[6–10] in quasi-two-dimensional (2D) superconductors. Related systems have been studied which involve thin layers of a superconducting element separated by some sort of "isolating" material, either an insulator,[8] a normal metal,[9] or even another superconductor with a lower T_c.[10] The use of an insulator minimizes the suppression of T_c via the proximity effect. It is a general property of these layered systems that as the isolating layer thickness becomes of the order of an interlayer coherence length $\xi_\perp(T)$ the superconducting layers become decoupled and exhibit properties determined by the individual layers. A dramatic demonstration is the sharp upturn of $H_{c2\parallel}(T)$ at a 2D-3D crossover temperature $T^* < T_c$.[3,8,9,11,12] Above T^*, $\xi_\perp(T)$ is larger than the superlattice repeat distance and the system exhibits 3D-like behavior of the parallel upper critical field where, in the Landau–Ginzburg regime,[2]

$$H_{c2\parallel}(T) = \phi_0/2\pi\xi_\parallel(T)\xi_\perp(T) \propto (1 - T/T_c); \quad (1)$$

here $\xi_\parallel$ is the in-plane coherence length and ϕ_0 is the flux quantum $hc/2e$.

At temperatures below T^*, a 2D behavior[4,11] is observed:

$$H_{c2\parallel}(T) = \phi_0/2\pi\xi_\parallel(T)(D_s/\sqrt{12}) \propto (1 - T/T_c)^{1/2}; \quad (2)$$

where D_s is the thickness of the superconducting film.

The above suggests that a considerable enhancement of $H_{c2\parallel}$ can be achieved for small superconducting layer thicknesses, as is often observed in practice.

In this paper, we report the synthesis and superconducting properties of sandwich and multilayer (superlattice) structures composed of the superconducting alloy $Nb_{0.53}Ti_{0.47}$ and amorphous Ge. The alloy $Nb_{0.53}Ti_{0.47}$ is a widely used high critical field superconductor[13] which is relatively ductile and compatible with copper. It has the advantages of greater metallurgical and cryogenic stability over the other commercially used conductor Nb_3Sn, but with the shortcoming of having an upper critical field of only 140 kG (at a temperature of 1.5 K). The diminished H_{c2} arises in part from the large Pauli paramagnetism of Nb-Ti which lowers the free energy of the normal state.[14,15] Although alloying of Nb-Ti with heavier elements (such as Ta or Hf) has been studied to relax the paramagnetic limit (via spin-orbit scattering processes),[15,16] the improvements have been minimal.

II. SAMPLE PREPARATION AND X-RAY ANALYSIS

The $Nb_{0.53}Ti_{0.47}$/Ge structures were prepared with a novel four-gun multisubstrate sputtering system.[17] With

 0021-8979/85/072543-07$02.40

four sputter guns, we can prepare superlattices such as A_xB_{1-x}/C_yD_{1-y} by cosputtering with guns containing each of the components A, B, C, and D. By monitoring the sputter rate of each gun, the compositions x and y can be easily controlled until the required stoichiometry is achieved. In this experiment, one of the unemployed guns is used to sputter Ti which acted as a sublimation pump during the film preparation process. The S-guns were supplied by Sputtered Films, Inc.

The $Nb_{0.53}Ti_{0.47}$ target was prepared by arc-melting the starting material (obtained from Kawecki Berylco Industries) to approximately the desired shape in a specially designed annular two-piece copper hearth which was then machined to the final tolerances. The Ge target was cast in its final form in an induction-heated graphite mold from 99.9999% pure starting material. The three substrate holders can be individually heated to over 1000 °C; the temperatures are monitored by Chromel/Alumel thermocouples. The substrate holders are mounted on a computer-controlled turntable. During deposition, the movement of the substrate holder is programmed to hover alternatively above the two guns containing the $Nb_{0.53}Ti_{0.47}$ and Ge targets. The period that the substrate remains above each of the targets, together with the deposition rates, determine the modulation wavelength or layer repeat distance of the structures.

The substrates used were 1/2×1/2×0.025-in., 0° sapphire and a layer of approximately 40 Å of Ge was deposited prior to depositing a superlattice. This was followed by the deposition of 60 layers of $Nb_{0.53}Ti_{0.47}$ and Ge, and then a final layer of 40 Å of Ge was deposited to protect the structure from atmospheric contamination. The deposition rates, which were monitored by two quartz sensors, were typically about 2 Å/s. The pressure of the argon gas was 5 mTorr and the purity was 99.999%.

The high angle θ-2θ diffractometer scan showed a textured growth of $Nb_{0.53}Ti_{0.47}$ layers with the bcc (110) planes parallel to the substrate; no indication of crystalline Ge peaks was seen for the range of substrate temperature studied (55–500 °C). The rocking curves of the (110) $Nb_{0.53}Ti_{0.47}$ peak for films deposited at different temperatures are shown in Fig. 1. The relative intensity suggested an optimum deposition temperature of about 200 °C. We note here that films deposited at 400 °C or above showed no texture at all. The films studied here were all grown at an indicated substrate temperature of 200 °C.

Low angle diffractometer scans are shown in Figs. 2(a) and 2(b) for two superlattices with different D_s/D_{Ge} ratios, where D_s and D_{Ge} are the layer thickness of $Nb_{0.53}Ti_{0.47}$ and Ge, respectively. The distinct low angle satellite peaks indi-

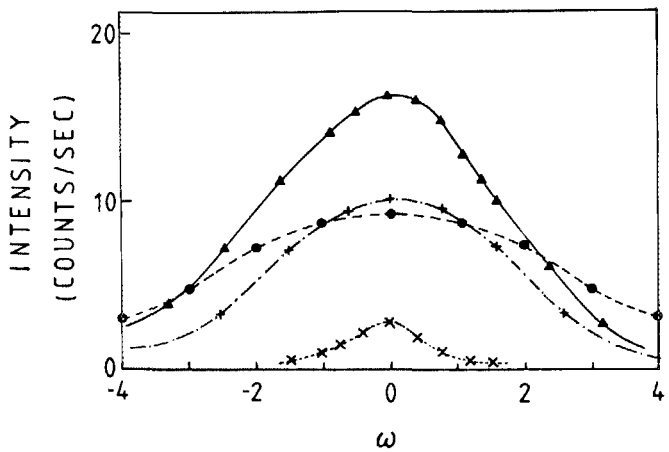

FIG. 1. The rocking curves of the $Nb_{0.53}Ti_{0.47}$ (110) peak of films deposited at varying temperatures with D_s/D_{Ge} = 60 Å/50 Å. ×: 40 °C; +: 100 °C; ▲: 140 °C; ●: 260 °C.

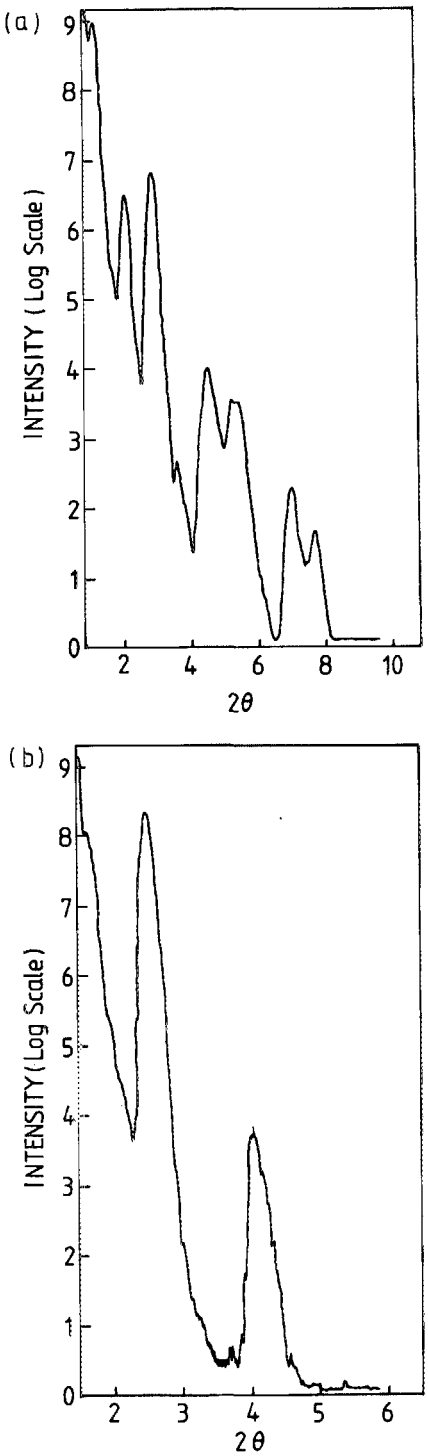

FIG. 2. The low angle diffractometer scan: (a) D_s/D_{Ge} = 60 Å/100 Å; (b) D_s/D_{Ge} = 0.5 Å/28 Å.

cate a high degree of periodicity in the direction normal to the layering, even for the $Nb_{0.53}Ti_{0.47}$ sublayer thickness as thin as 0.5 Å. The modulation wavelength $S = D_s + D_{Ge}$ can be calculated with the following equation[18]:

$$S = \lambda/2(\Delta\theta), \tag{3}$$

where λ is the x-ray wavelength of CuKα radiation, (1.54 Å) and $\Delta\theta$ is the separation between neighboring low angle satellites. The individual layer thicknesses D_s and D_{Ge} are determined by solving a set of linear equations,

$$S_i = \alpha_i r_{A_i}(t_{A_i} + \Delta t) + \beta_i r_{B_i}(t_{B_i} + \Delta t) = D_s + D_{Ge}, \tag{4}$$

where α_i, β_i are geometric tooling factors: r_{A_i}, r_{B_i} are the deposition rates for $Nb_{0.53}Ti_{0.47}$ and Ge (as read by the quartz sensors), t_{A_i} and t_{B_i} are the times the holder stays above the $Nb_{0.53}Ti_{0.47}$ and Ge targets, respectively, and Δt is the time needed for the holder to clear the shutter opening (which is usually negligible for larger t_{A_i} and t_{B_i}).

The values of D_s calculated by Eq. (4) were compared with those calculated with the Scherr formula,

$$D_s = \frac{0.9\lambda}{B\cos\theta}, \tag{5}$$

where $B = \sqrt{B_m^2 - B_s^2}$, B_m is the FWHM of the $Nb_{0.53}Ti_{0.47}$ (110) peak, and $B_s \sim 0.18°$ is the instrumental broadening; the two were found to differ by about 10% for D_s in the range of 50 to 90 Å and by about 30% for thickness larger than 120 Å. In this experiment, we consistently used Eq. (4) to calculate D_s.

III. TRANSPORT PROPERTIES

The temperature dependence of the sheet resistance per layer ($R_\square$) of our samples was measured with the four-probe method on photolithographically defined samples. The width of the samples was 0.5 mm and the distance between the potential leads was 2.83 mm. Measurements were performed with a variable temperature susceptometer, SHE VTS-805, which provides magnetic fields to 50 kG and temperatures from 1.8 to 400 K. Table I shows some properties of films with varying $Nb_{0.53}Ti_{0.47}$ thicknesses.

We note here that at a temperature of 1.8 K, the superlattice with the thinnest metal layer thickness (D_s/D_{Ge} = 0.5 Å/28 Å) has a resistance 10^4 times smaller than a similarly prepared pure Ge film with about the same total thickness. This indicates that the conductivity is mainly due to the metal layers in the superlattices.

TABLE I. Physical properties of $Nb_{0.53}Ti_{0.47}$/Ge superlattices.

D_s/D_{Ge} (Å/Å)	$R_\square$ (Ω)	T_c (K)	R (300 K)/R (20 K)
0.5/28	2.2×10^5	...	0.27
0.9/28	4.8×10^3	...	0.72
1.6/27	2.1×10^3	...	0.90
3/30	1.6×10^3	...	0.85
7.5/30	984	...	0.88
15/29	627	...	0.95
38/45	298	2.51	0.98
42/49	296	2.65	0.97
59/38	196	5.10	1.03
89/38	99	6.60	1.06
129/38	66	7.60	1.15
144/32	61	7.58	1.09
163/28	51	7.94	1.09
221/45	47	8.91	1.14

TABLE II. Physical properties of $GeNb_{0.53}Ti_{0.47}$/Ge sandwich films.

$D_{Ge}/D_s/D_{Ge}$ (Å/Å/Å)	$R_\square$ (Ω)	T_c (K)	R (300 K)/R (20 K)
300/0.5/300	2.35×10^5	...	0.32
300/33/300	340	...	0.97
300/50/300	201	3.94	1.00
300/100/300	78	6.77	1.08
300/1000/300	6	9.16	1.15

To compare the properties of a superlattice with those of a single layer of $Nb_{0.53}Ti_{0.47}$, we have also prepared single layer $Nb_{0.53}Ti_{0.47}$ films with a thick Ge layer on each side; the properties of these sandwich films are listed in Table II.

The sheet resistance $R_\square$ is plotted in Fig. 3; note that it is inversely proportional to D_s for films with D_s larger than ~40 Å, suggesting an approximately uniform resistivity in the individual $Nb_{0.53}Ti_{0.47}$ layer, i.e.,

$$\rho = R_\square D_s \simeq 90\,\mu\Omega\text{ cm}. \tag{6}$$

This is close to the bulk value of 80 $\mu\Omega$ cm. For films with D_s < 40 Å, $R_\square$ deviates from a D_s^{-1} dependence in the direction of lower resistivity. This is attributed to the effect of superconducting fluctuations[19] which are more important for layered superconductor with shorter mean free paths (i.e., more disorder). The superconducting fluctuations can extend to a temperature of the order of $T \sim 2T_c$ for highly disordered superlattice superconductors. On the other hand,

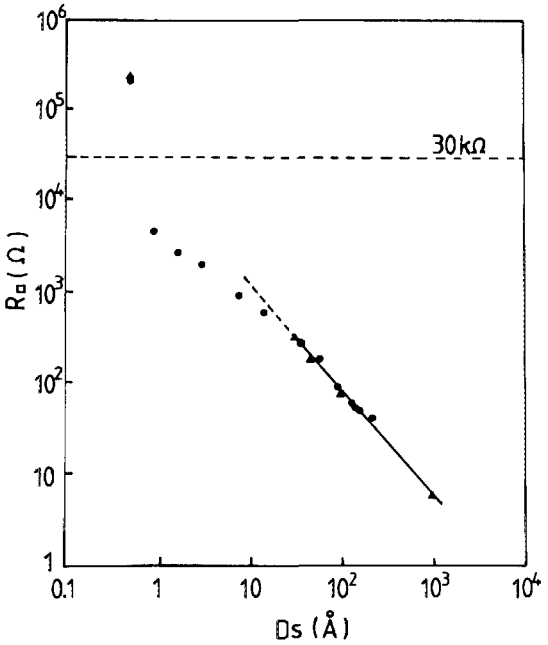

FIG. 3. Resistance per square ($R_\square$) vs the $Nb_{0.53}Ti_{0.47}$ layer thickness (D_s). ●: $Nb_{0.53}Ti_{0.47}$ superlattice; ▲: Ge/$Nb_{0.53}Ti_{0.47}$/Ge sandwich.

note that when D_s is decreased from 0.9 to 0.5 Å, the sheet resistance increased abruptly from 4.8 to 220 kΩ, implying a transition from a weakly localized state to a strongly localized state; this is consistent with theoretical predictions of a mobility edge near $R_\square \approx \pi^2\hbar/e^2 \approx 30$ kΩ.[20] This interpretation is strengthened by our observation of a transition from a logarithmic to an exponential temperature dependence of the resistance; these and other properties relating to so called localization[21] and interaction[22] effects will be discussed in a separate paper.[23] In Fig. 3, the D_s dependence of the sheet resistance of five of the sandwich samples is also plotted and found to be perfectly compatible with the superlattice data, which suggests a quasi-2D nature for our multilayer films.

IV. SUPERCONDUCTING PROPERTIES

A. Critical temperatures T_c

We have observed a sharp decrease of the superconducting transition temperature with increasing sheet resistance (see Fig. 4). A similar degradation of T_c has been observed in other two-dimensional thin film[24,25,26] systems and was attributed to the inherent competition between superconductivity and the disorder-related localization and Coulomb interaction effects. Maekawa and Fukuyama[27] have recently investigated the effect of localization in two-dimensional superconductors and obtain an expression in terms of the sheet resistance,

$$\ln(T_c/T_{c_0}) = \frac{(g_1 - 3g')N(0)e^2R_\square}{4\pi^2\hbar}\left[\ln\left(5.40\frac{\xi_0}{l}\frac{T_{c_0}}{T_c}\right)\right]^2 - \frac{(g_1 + g')N(0)e^2R_\square}{6\pi^2\hbar}\left[\ln\left(5.40\frac{\xi_0}{l}\frac{T_{c_0}}{T_c}\right)\right]^3, \quad (7)$$

where g_1 and g' are the exchange and self-energy interaction strengths, respectively; $N(0)$ is the density of states; ξ_0 is the superconducting coherence length of pure material; l is the mean free path; and T_{c_0} is the bulk superconducting transition temperature. To fit the experimental data using Eq. (7), we used the Nb coherence length of 380 Å for ξ_0 and the approximate interatomic spacing, 3 Å, for the mean free path; although somewhat arbitrary, the values chosen are of the correct order of magnitude. The constant g' is usually small compared to g_1 and will be neglected. The remaining parameter $g_1N(0) \sim 2.0$ is then obtained by linear regression. The large value of $g_1N(0)$ indicates the existence of strong electron-electron interaction effects in these quasi-2D superconductors. The T_c curve calculated with the M–F theory exhibits a minimum around 0.4 K. The predicted reentrance can only be observed below 0.4 K and with samples having a sheet resistance between 330 and 360 Ω. It is apparently not clear at this time whether the reentrant phenomena is an artifact of the theory or is, in fact, observable.

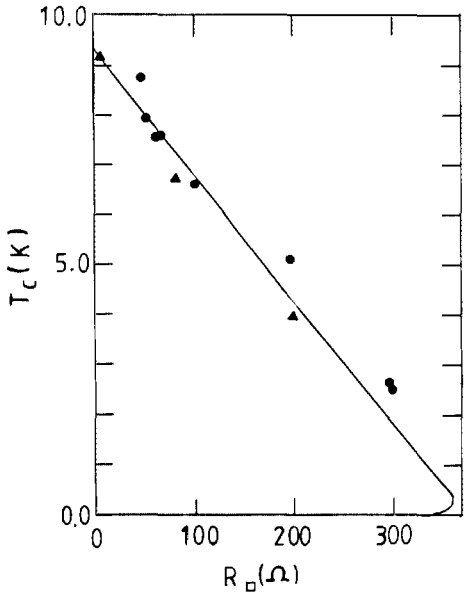

FIG. 4. T_c vs $R_\square$. The solid curve is from the Maekawa–Fukuyama theory. ●: superlattices; ▲: sandwiches.

B. Upper critical field

Both the parallel $H_{c2\parallel}(T)$ and perpendicular $H_{c2\perp}(T)$ critical fields were measured with magnetic fields up to 50 kG. The results are shown in Figs. 5(a) and 5(b) for films with

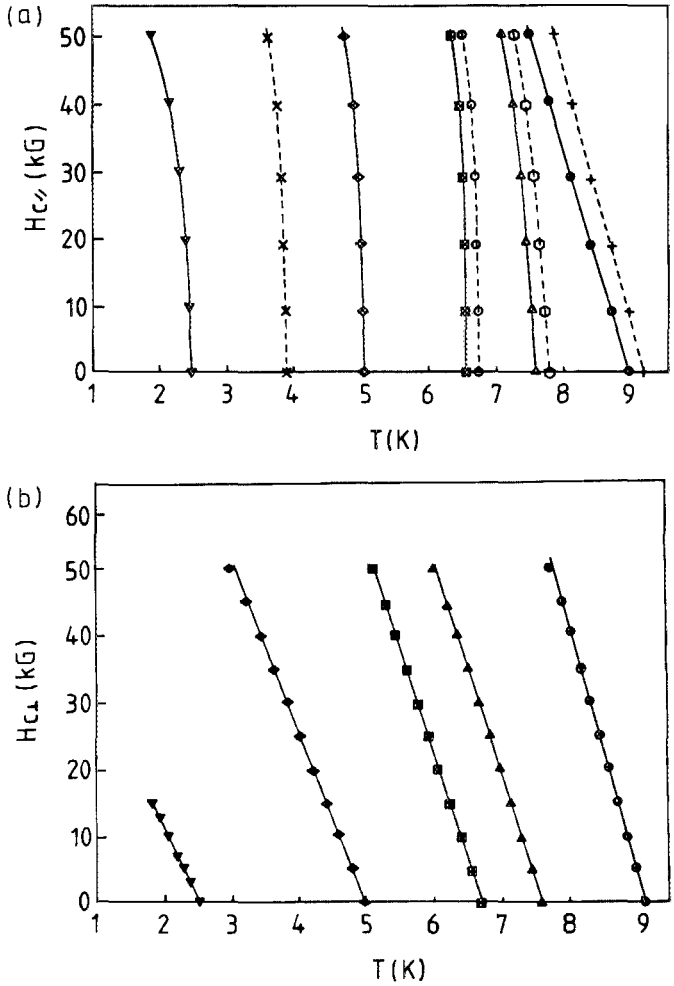

FIG. 5. (a) $H_{c2\parallel}(T)$ vs T. The solid lines are for superlattices and the dashed lines for sandwiches. The following notation is employed: For the superlattice the D_s(Å)/D_{Ge}(Å) values are ▼, 48/45; ◆, 59/38; ■, 89/38; ▲, 144/38; ●, 221/94. For the sandwiches the D_{Ge}(Å)/D_s(Å)/D_{Ge}(Å) values are ×, 300/33/300; ○, 300/50/300; ○, 300/100/300; +, 300/1000/300. (b) $H_{c2\perp}(T)$ vs T. The symbol used for each sample is the same as that used in Fig. 5(a).

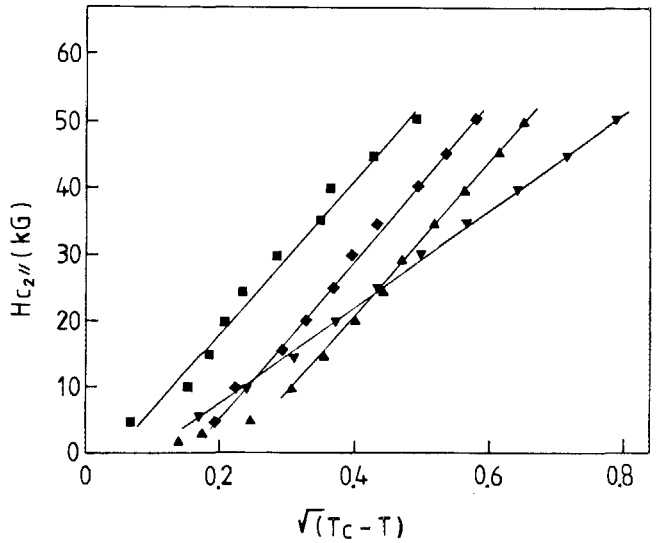

FIG. 6. $H_{c2\parallel}(T)$ vs $(T_c - T)^{1/2}$. Notations are the same as those used in Fig. 5(a).

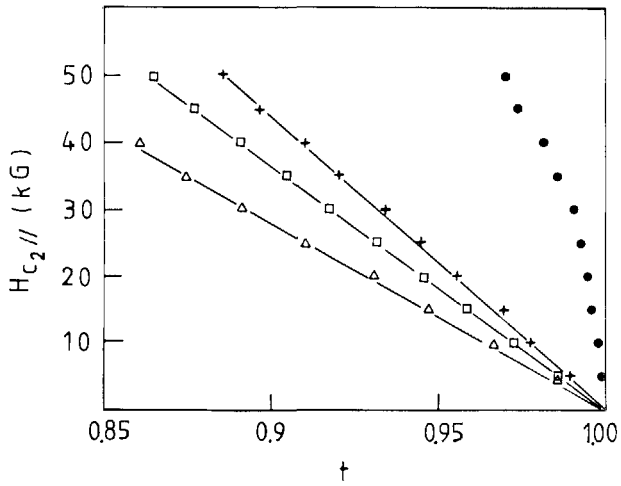

FIG. 7. $H_{c2\parallel}(T)$ vs t, where $t \equiv T/T_c$ is the reduced temperature for films with fixed $Nb_{0.53}Ti_{0.47}$ thickness (95 Å) and the following Ge thicknesses: ●, 45 Å; +, 10 Å, □, 15 Å; △, 20 Å.

relatively thick Ge layers and varying $Nb_{0.53}Ti_{0.47}$ thicknesses. All the perpendicular critical fields shown in Fig. 5(b) are linear in T as expected from theory.[2] For a dirty isotropic type II superconductor,[28] we have

$$H_{c2\perp}(T) = 0.22 \frac{\phi_0}{\xi_0 l} \frac{T_c - T}{T_c}. \tag{8}$$

The parameter $(\xi_0 l)^{1/2}$ calculated from the slope of the $H_{c2\perp}(T)$ line (thick D_s sample) is 37 Å and compares well with the value used in fitting the T_c curves (34 Å). In Fig. 5(a), we see a rapid (nearly vertical) rise in $H_{c2\parallel}(T)$ for films with $D_s \leqslant 200$ Å. We have also plotted $H_{c2\parallel}(T)$ vs $(T_c - T)^{1/2}$ in Fig. 6. The linear dependence of $H_{c2\parallel}(T)$ on $(T_c - T)^{1/2}$ is in agreement with the prediction of Eq. (2) and clearly shows the quasi-2D nature of our films when $D_s \leqslant 200$ Å. The measurements on the sandwich samples are shown in the dashed lines in Fig. 5(a) and are, again, consistent with the superlattice samples. The departure from the expected behavior near T_c is usually ascribed to sample inhomogeneities.

The zero temperature critical field $H_{c2\parallel}(0)$ for thin films has been studied by various investigators[29–31] with differing results depending on the relative size of the lengths D_s, ξ_0, and l. Since our superconducting films all have layer thicknesses larger than 40 Å, we will use the Rickayzen theory[31] which is applicable when $l \ll (l\xi_0)^{1/2} < D_s$.

TABLE III. Zero temperature parallel upper critical field estimated with the Rickayzen formula.

D_s/D_{Ge} (Å/Å)	T_c (K)	$H_{c2\parallel}(0)$ (kG)
164/28	7.82	329
144/32	7.58	400
129/38	7.55	344
89/38	6.59	391
59/38	5.09	347
48/45	2.51	148

The parallel critical fields given by Rickayzen in two limiting cases are as follows,

$$H_{c2\parallel}(T \to T_c) = \frac{6c\hbar}{eD_s} \left(\frac{2k\Delta T}{\hbar w_F l \pi}\right)^{1/2} \tag{9}$$

and

$$H_{c2\parallel}(T = 0) = \frac{c\hbar}{eD_s} (\exp 1) \left[\frac{3\pi k T_c}{\gamma \hbar w_F l}\right]^{1/2}, \tag{10}$$

where $\Delta T = T_c - T$, $\gamma = 1.781$, v_F is the Fermi velocity, and D_s is the layer thickness. Combining Eqs. (9) and (10), we obtain

$$H_{c2\parallel}(T = 0) \simeq 1.306 \sqrt{T_c} \left(\frac{dH}{d(\sqrt{T_c - T})}\right)_{T \to T_c}, \tag{11}$$

where the quantity in large parentheses is just the slope of the $H_{c2\parallel}(T)$ vs $(T_c - T)^{1/2}$ curve near T_c. The zero temperature $H_{c2\parallel}$ values estimated by Eq. (11) are listed in Table III. We see from this table that $H_{c2\parallel}(0)$ reaches a maximum of 400 kG for films with Nb-Ti layer thicknesses of 144 Å. The quasi-2D behavior of $H_{c2\parallel}(T)$ vanishes when either the Nb-Ti layer thickness becomes larger than 200 Å [see Fig. 5(a)] or the thickness of the Ge layers is reduced to the point where substantial Josephson coupling between the superconducting layers occurs (typically around 20 Å). The latter case was observed and is shown in Fig. 7.

C. The critical current density

For practical applications, it is desirable to know the critical current density as a function of temperature and applied field. Only one sample was studied in the present work. Time isolated pulses (of 3 μs length) were applied to the sample in series with a 2.186-Ω resistor, the latter being used to determine the sample current. The pulse width was restricted in order to avoid heating of the sample. A dual trace oscilloscope was used to individually measure the voltage drop across the sample and the current sensing resistor. The pulse height was then gradually increased until the sample current decreased by about 0.3%; this is equivalent to about

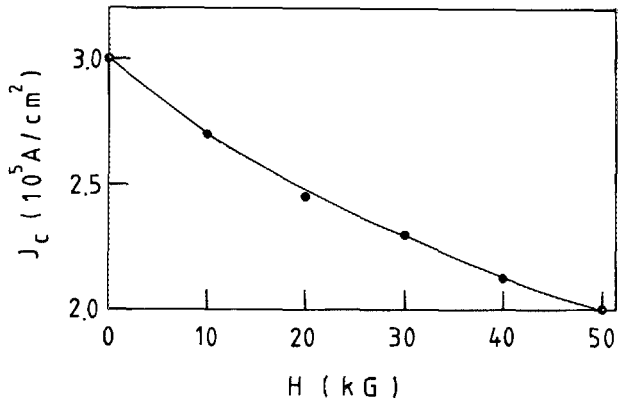

FIG. 8. Critical current density vs external field at $T = 1.8$ K for $D_s/D_{Ge} = 89$ Å/38 Å.

a 5-mV voltage on the sample, and was observed as an amplitude shift between the leading and trailing edges of the pulse. The critical current is then taken as the onset current for this phenomenon. The results are shown in Figs. 8 and 9. We note that the critical current density (1.2×10^5 A/cm^2) at 50 kG and 4.2 K is comparable to the bulk $Nb_{0.53}Ti_{0.47}$ value[32] ($1.8\sim2.0\times10^5$ A/cm^2).

V. CONCLUSIONS

Very good quality multilayer films of $Nb_{0.53}Ti_{0.47}$/Ge have been prepared in a controlled manner with the programmable deposition process described in this work. The parallel upper critical field was studied in both the 2D and 3D regions by systematically varying the $Nb_{0.53}Ti_{0.47}$ and Ge layer thicknesses. $H_{c2\|}(0)$ was estimated with the Rickayzen formula and found to be 2.7 times higher than the bulk value. The Rickayzen formula does not include the effect of localization and Coulomb interactions on the upper critical field[33,34] which could well be important. It also does not include the paramagnetic limiting nor spin-orbit scattering effects. Thus, the estimated value of $H_{c2\|}(0)$ should be treated cautiously; however, it is apparent that a considerable increase in $H_{c2\|}$ can be achieved by layering with a second insulating component.

One might well question the utility of a high $H_{c2\|}$ when the $H_{c2\perp}$ values are substantially lower. Here we simply point out that by properly tilting the plane of a multilayer ribbon to be parallel to the local direction of the field at each point in a magnet, the full value of $H_{c2\|}$ can be realized; this could be accomplished in practice by the occasional insertion of appropriately shaped packing material while winding the magnet. To obtain cryogenic stability, multilayer films composed of stacks of ...$Nb_{0.53}Ti_{0.47}$/Ge/Cu/Ge... may be easily fabricated with our four-gun system and will hopefully be the subject of future studies.

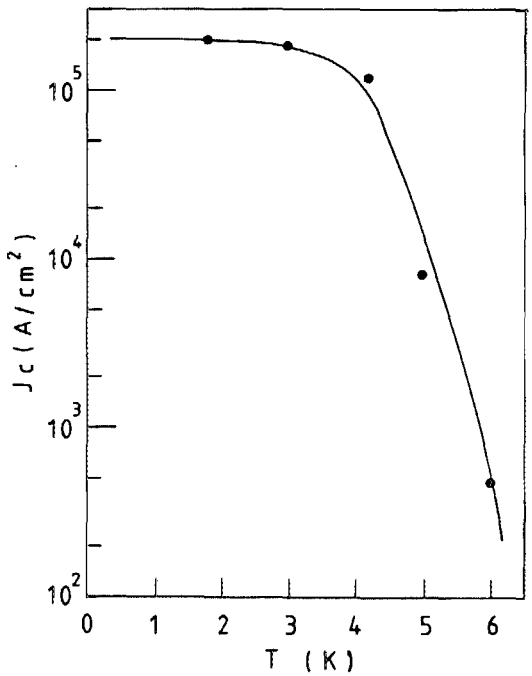

FIG. 9. Critical current density vs temperature at an applied field of 50 kG for $D_s/D_{Ge} = 89$ Å/38 Å.

ACKNOWLEDGMENTS

This research was supported by the Office of Naval Research under grant N00014-82-K-0598; the Northwestern Materials Research Center under NSF grant DMR-82-16972, and by the U. S. Department of Energy through Argonne National Laboratory.

[1]F. R. Gamble, F. J. Di Salvo, R. A. Klemm, and T. H. Geballe, Science **168**, 568 (1970).
[2]W. E. Lawrence and S. Doniach, in *Proceedings of the 12th International Conference on Low Temperature Physics*, edited by E. Kanda (Academic Press of Tokyo, Kyoto, Japan, 1971), pp. 361-362.
[3]R. A. Klemm, A. Luther, and M. R. Beasley, Phys. Rev. B **12**, 877 (1975).
[4]G. Deutscher and O. E. Wohlman, Phys. Rev. B **17**, 1249 (1978).
[5]K. Takanaka, J. Phys. Soc. Jpn. **52**, 2173 (1983).
[6]J. A. Woollam and R. B. Somoano, Phys. Rev. B **13**, 3854 (1976).
[7]T. W. Haywood and D. G. Ast, Phys. Rev. B **18**, 2225 (1978).
[8]S. T. Ruggiero, T. W. Barbee, M. R. Beasley, Phys. Rev. B **26**, 4849 (1982).
[9]I. Banerjee, Q. S. Yang, C. M. Falco, and I. K. Schuller, Solid State Commun. **41**, 805 (1982).
[10]Y. J. Qian, J. A. Zheng, B. K. Sarma, H. Q. Yang, J. B. Ketterson, and J. E. Hilliard, J. Low Temp. Phys. **49**, 805 (1982).
[11]D. Saint-James and P. G. de Gennes, Phys. Lett. **7**, 306 (1963); F. E. Harper and M. Tinkham, Phys. Rev. **172**, 441 (1968).
[12]H. K. Wong, B. Y. Jin, H. Q. Yang, J. B. Ketterson, and J. E. Hilliard, International Conference on Superlattices, Microstructures, and Microdevices. Champaign-Urbana, IL, August 1984.
[13]H. R. Segal, K. Hemachalam, T. A. De Winter, and Z. J. J. Stekley, IEEE Trans. Magn. **MAG-15**, 807 (1979).
[14]B. S. Chandrasekar, Appl. Phys. Lett. **1**, 7 (1962); A. M. Clogston, Phys. Rev. Lett. **9**, 266 (1962).
[15]D. G. Kawksworth and D. C. Larbalestier, IEEE Trans. Magn. **MAG-17**, 49 (1981).
[16]N. R. Werthamer, E. Helfand, and P. C. Hohenberg, Phys. Rev. **147**, 295 (1966).
[17]H. Q. Yang, B. Y. Jin, Y. H. Shen, H. K. Wong, J. E. Hilliard, and J. B. Ketterson, (submitted to Rev. Sci. Instrument).
[18]D. de Fontaine, in *Local Atomic Arrangements Studied by X-Ray Diffraction*, edited by J. B. Cohen and J. E. Hilliard (Gordon and Breach, New York, 1966), p. 51.
[19]L. G. Aslamasov and A. A. Varlamov. J. Low Temp. Phys. **38**, 223 (1980).
[20]D. C. Liciardello and D. J. Thouless, J. Phys. C. **8**, 4157 (1975); P. A. Lee, Phys. Rev. Lett. **42**, 1492 (1979).
[21]E. Abraham, P. W. Anderson, D. C. Liciardello, and T. V. Ramakirhsnan, Phys. Rev. Lett. **42**, 673 (1979).
[22]B. L. Altshuler, A. G. Aronov, and P. A. Lee, Phys. Rev. Lett. **44**, 1288

(1980).
[23]B. Y. Jin, Y. H. Shen, H. Q. Yang, H. K. Wong, J. E. Hilliard, and J. B. Ketterson; International Conference on Superlattices, Microstructures, and Microdevices. Champaign-Urbana, IL, August 1984.
[24]S. Mohlecke and Z. Ovadyahu; Phys. Rev. B **29**, 6203 (1984).
[25]H. Raffy, R. B. Laibowitz, P. Chaudhari, and S. Maekawa; Phys. Rev. B **28**, 6607 (1983).
[26]J. M. Graybeal and M. R. Beasley, Phys. Rev. B **29**, 4167 (1984).
[27]S. Maekawa and H. Fukuyama, J. Phys. Soc. Jpn. **51**, 1380 (1981).
[28]P. G. De Gennes, *Superconductivity in Metals and Alloys* (Benjamin, New York, 1966).
[29]Y. Nambu and S. F. Tuan, Phys. Rev. **133**, A1 (1964).
[30]K. Maki, Prog. Theor. Phys. (Kyoto) **29**, 603 (1963).
[31]G. Rickayzen, Phys. Rev. **138**, A73 (1965).
[32]D. C. Larbalestier, Adv. Cryog. Eng. **26**, 10 (1980).
[33]S. Maekawa, H. Ebisawa, H. Fukuyama; J. Phys. Soc. Jpn. **52**, 1352 (1983).
[34]L. Coffey, K. A. Muttalib, and K. Levin, Phys. Rev. Lett. **52**, 783 (1984).